Supporting information for the article:

From iron curtain to green belt: Elbe River shift from heterotrophic to autotrophic nitrogen retention over 35 years of passive restoration

Alexander Wachholz[1], James W Jawitz[2], Dietrich Borchardt[1]

1. Segment geometry estimation

a. Travel time model

We employ the travel time model introduced by Scharfe et al. (2009) to estimate the travel time (τ) in the Elbe River:

(I) $$\tau(t) = \frac{Q_{ref}^{\frac{\tau_{ref}}{3}}}{Q(t)}$$

where Q_{ref} is 270 m^3/s, and τ_{ref} is 240 hours. While this model was developed for the entire German Elbe (585 km), we assume the flow velocity is distributed homogeneously and adjust it for the length of our segment (111 km).

b. Channel area model

To predict channel area (*A*), we use a power law relationship, $A(t) = aQ(t)^b$, between discharge (*Q*) and channel area (Booker and Dunbar, 2008). To parameterize this relationship, we apply the Normalized Difference Water Index (NDWI) algorithm (Gao, 1996) on Sentinel 2 images with a 10-meter resolution, taken during various discharge conditions (186-1020 $m^3\ s^{-1}$) and with a maximum of 10% cloud cover over the study area.

c. Channel depth model

To predict channel depth (Z), we also use a power law relationship of the form $Z(t)=aQ(t)^b$ (Modi et al., 2022). We fit the parameters based on data from the Elbe (Aberle et al., 2010).

2. Gaussian error propagation

We use gaussian error propagation to quantify the uncertainty for the mass balance estimates

(II) $$\sigma_{R_{obs}} = \sqrt{\sigma_{Lin}^2 + \sigma_{Lout}^2}$$

where σ is the absolute error of any term. The errors in L result from the errors in C and Q

(III) $$\sigma_L = \sqrt{\sigma_C^2 Q^2 + \sigma_Q^2 C^2}$$

for σ_C and σ_Q we assume a constant value of 10 % of the current C or Q value. We did not assess R_{obs} on days where Q was larger than the 90th flow percentile or where $\frac{Q_{in} - Q_{out}}{Q_{in}}$ was larger than 0.05 (18 % of all days). This led to an exclusion of 18 % of all dates, most of which (84%) occurred during high flows winter.

3. Interpolation of hourly dissolved oxygen time series

As daily DO curves are usually sinusoidal (Correa-González et al., 2014) and data from the Elbe confirms this general assumption (Kamjunke et al., 2021; their Fig. 5) we use a sine wave based approach to interpolate hourly DO concentrations from observed daily minimum, maximum, and mean values. We use a sine wave of the form

(IV) $$y(x) = mean + amplitude * \cos\left(\frac{2\pi}{period}(x - phase)\right)$$

and base the parameters *mean*, *amplitude*, *period* (τ), and *phase* (ϕ) on the measured DO concentrations

(V)

$$DO(hour) = DO_{mean}(day) + \frac{DO_{max}(day) - DO_{min}(day)}{2} \cos\left(\frac{2\pi}{\tau(day)}\left(hour - \frac{\phi(day)}{24}\tau(day)\right)\right)$$

where τ is the period of the sine chosen to satisfy that $\tau/2$ is the time between the peak (ϕ) and low (ψ) of DO concentrations. ϕ and ψ, however, are only available for 25 % of all days (n≈2000), so we derived transfer functions (Fig. S6a, b) that estimates τ and ϕ for each day of the year based on daylight hours (time between sunrise and sunset).

(VI) $$\tau(day) = 2(i + m * daylight\,hours)$$

As ϕ follows a sinusoidal curve itself during the year, we approximate it using a sine function

(VII) $$\phi(day) = 16 + 2\cos\frac{2\pi}{365}(\text{day-}180))$$

This approach leads to dates where the period of the sine τ is less than 24 hours (especially during winter), which means less than 24 hours of DO concentrations are simulated. We use linear interpolation for missing hours, filling a maximum of 12 consecutive hours. We validate this approach by comparing the simulated hourly DO concentrations with 2 years (2015, 2016) high frequency (30-minute) sensor measurements from the same site (Fig. S7) provided by the Niedersächsischer Landesbetrieb für Wasserwirtschaft, Küsten- und Naturschutz (NLWKN).

4. Metabolism model implementation and validation

We estimated gross primary production (gpp), ecosystem respiration (er), and the light use efficiency (k600) by solving Eq. 4 using a Bayesian inference approach with Monte Carlo Markov Chain (MCMC) simulations. For gpp and er, we used minimally informed priors $N\sim(\mu=5, \sigma=10)$ based on a previous study (Hall et al., 2016). To define the priors for k600, we used unpublished estimations from another study in the Elbe and set them to $N\sim(\mu=6, \sigma=2)$. We ran the model for each day using 4 chains with 10,000 iterations and a burn-in phase of 1,000, aiming for an acceptance rate of 20%. To assess the likelihood of each iteration, we compared the observed and simulated hourly DO changes, assuming that the errors were distributed according to a half-Cauchy distribution with a scale of 10. We use the mean and standard deviation of the resulting accepted gpp, er, and k600 values for further analysis. The MCMC model was implemented using the Python package *pymc3* (Salvatier et al., 2016).

We estimated *gpp*, *er*, and K600 for 9770 days in the Elbe main stream. Even though we selected wide priors for *gpp* and *er*, only 2.6 % of days resulted in negative estimations. Over the entire time series, k600 shows a clear seasonal pattern oscillating between 0 (August) and 5 (March) m d^{-1} while the amplitude slightly increases (Fig. S8). This was also reported by Arroita et al. (2019) following improvements in water quality caused by improved wastewater treatment. On 16 % of all days, k600 was negative, and those days occurred when residence times, water temperatures were high and DO_{sat} is > 100% (Fig. S8).

Regarding the goodness of fit of the Bayesian model, there was no trend in R^2 values over the time series (median 0.86). During winter, R^2 tends to be lower (median = 0.5) than during the rest of the year (Fig. S10a). However, the daily variability of DO is lower during winter, leading to low root mean square errors (median > 0.35 mmol m^{-3} day^{-1}) during winter seasons (Fig. 11c).

For further analyses, we only consider gpp, er, and k600 estimates from dates with non-negative GPP and ER values, where the RMSE is < 0.35 g O_2 m^{-3} day^{-1} or the R^2 value is higher than 0.75 (7940 days or 81 %). GPP estimations from our study are similar to findings from (Kamjunke et al., 2021), who found GPP peaks of 20 g O_2 m^{-2} day^{-1} for the Elbe during summer.

An important consideration when interpreting metabolic estimates is the areal extent over which the single station method integrates. Following Chapra and Di Toro (1991), this can be estimated as follows

(IX) $$ae = \frac{3v}{k600\, z}$$

where v is the flow velocity [m d^{-1}], *k600* is the gas exchange coefficient [m d^{-1}] and z is the channel depth [m]. By using median the median flow velocity (74.000 m d^{-1}), median k600 (2.9 m d^{-1}), and median channel depth (2.8 m), we arrive at an areal extent of 196 km covered by this approach, which is 76 % longer than the investigated segment. However, Kamjunke et al. (2022) showed that ER and NPP rates did change relatively little during the last 200 km of the Elbe compared to its entire length during periods of high biological activity, so we assume the single station metabolism estimation reflects the spatial scale of the DIN balance.

5. Figures

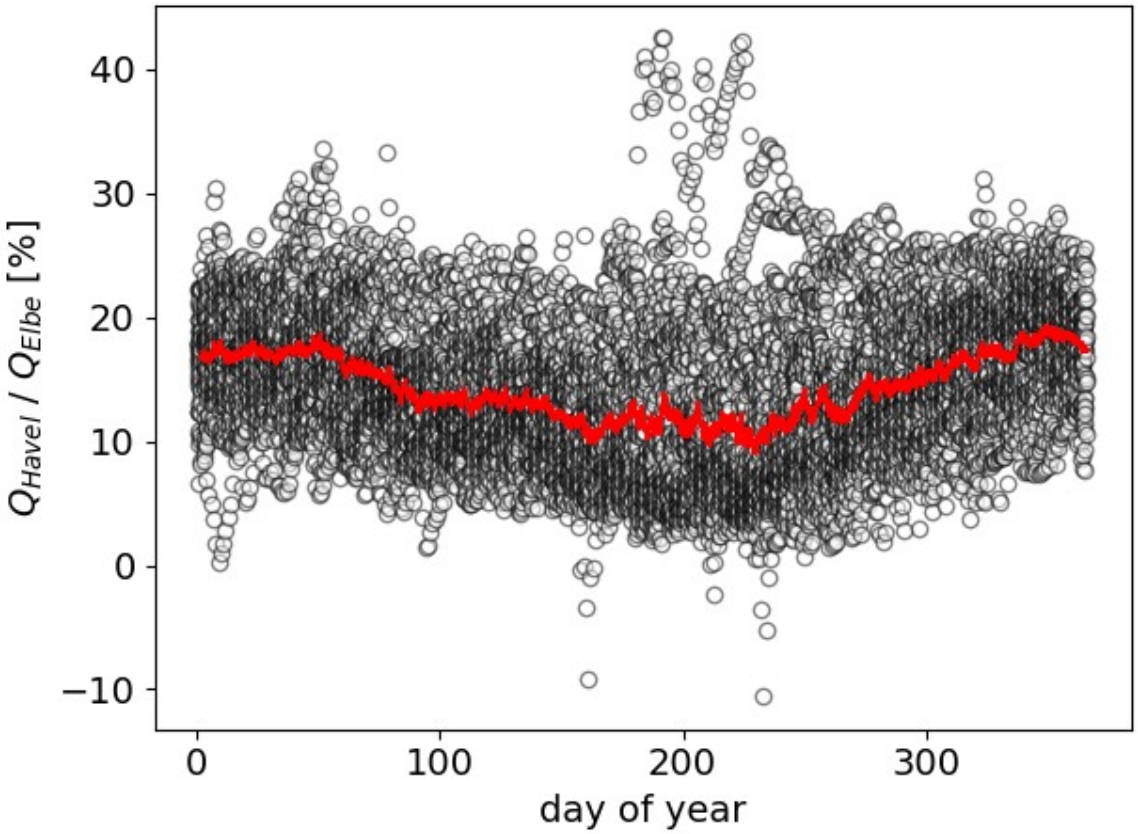

Figure S1. Fraction of the Havels (Gage: Havelberg-Stadt) discharge divided by the discharge of the Elbe (Gage: Neu-Darchau) (Fig.1a, b). Circles show raw data, and the red line is the multi-year mean for each day.

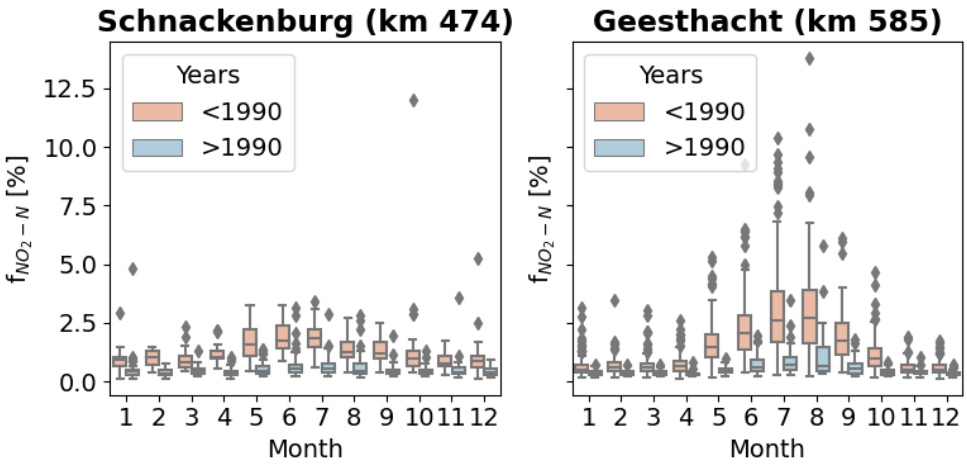

Figure S2: Fraction of NO2-N from dissolved inorganic DIN for the input (Schnackenburg) and output (Geesthacht) sampling sites of the mass balance in %.

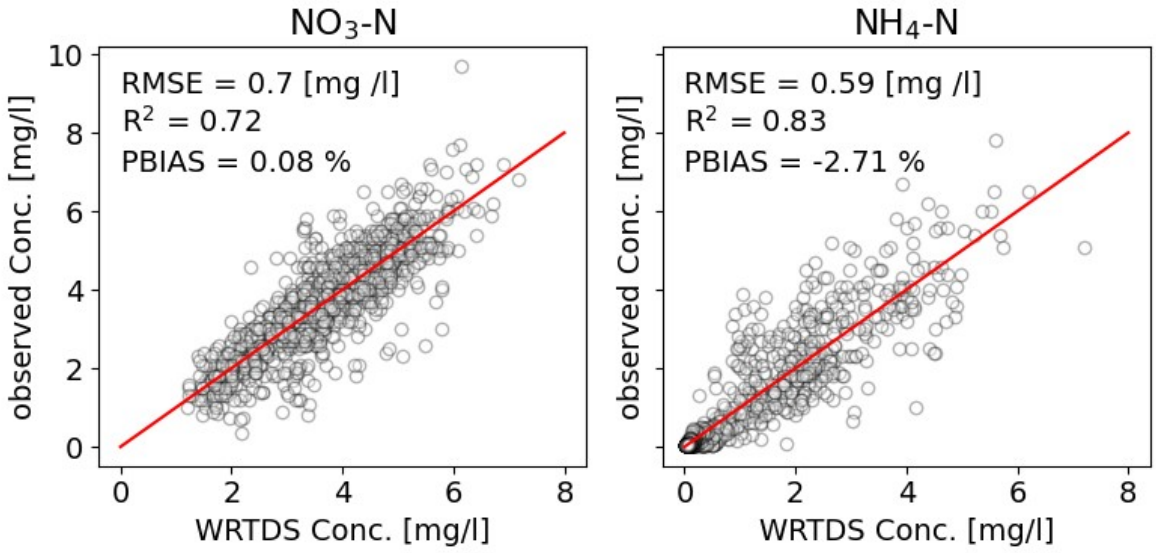

Figure S3: Measured vs WRTDS simulated daily N concentrations for the Elbe at the outlet of the investigated river segment (Geesthacht).

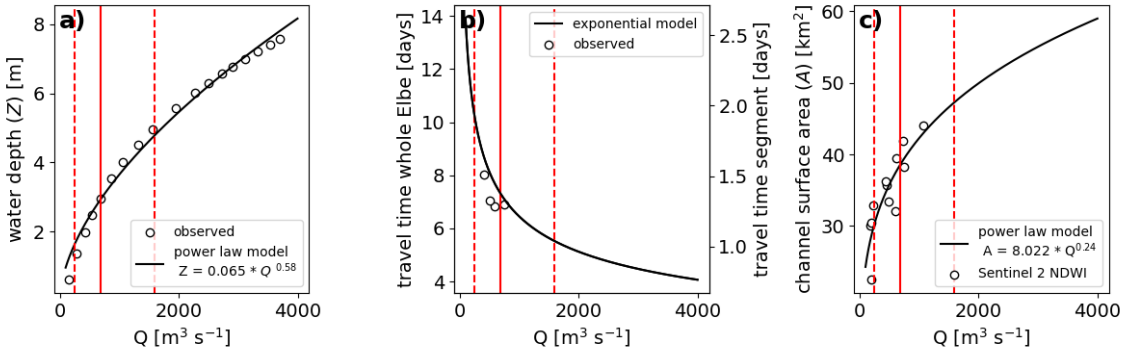

Figure S4. The discharge-based transfer function for channel depth, travel time, and channel surface area. The dashed red lines show the 5th and the 95th, and the solid red line shows the 50th flow percentile for the period 1978-2021 from the Gage Neu Darchau. In panel b), both the travel time along the entire Elbe (left y-axis) and the travel time along the investigated segment (right y-axis) are shown.

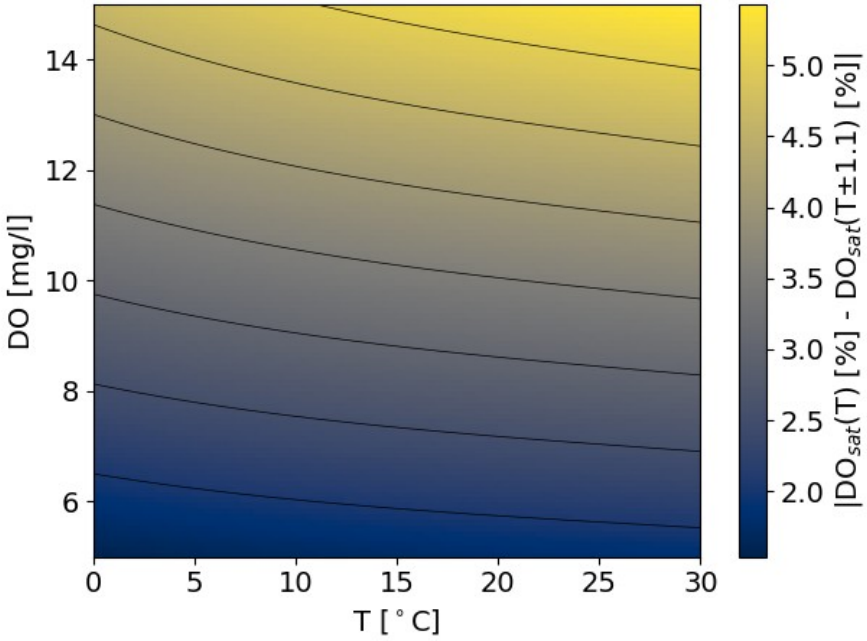

Figure S5. Maximal effect a temperature (T) error of 1.1 deg C can have on dissolved oxygen (DO) saturation for usual DO concentrations and temperatures in the river Elbe. Saturations were calculated using the Weiss Formula (Weiss, 1970) assuming a constant air pressure of 1020 hPa.

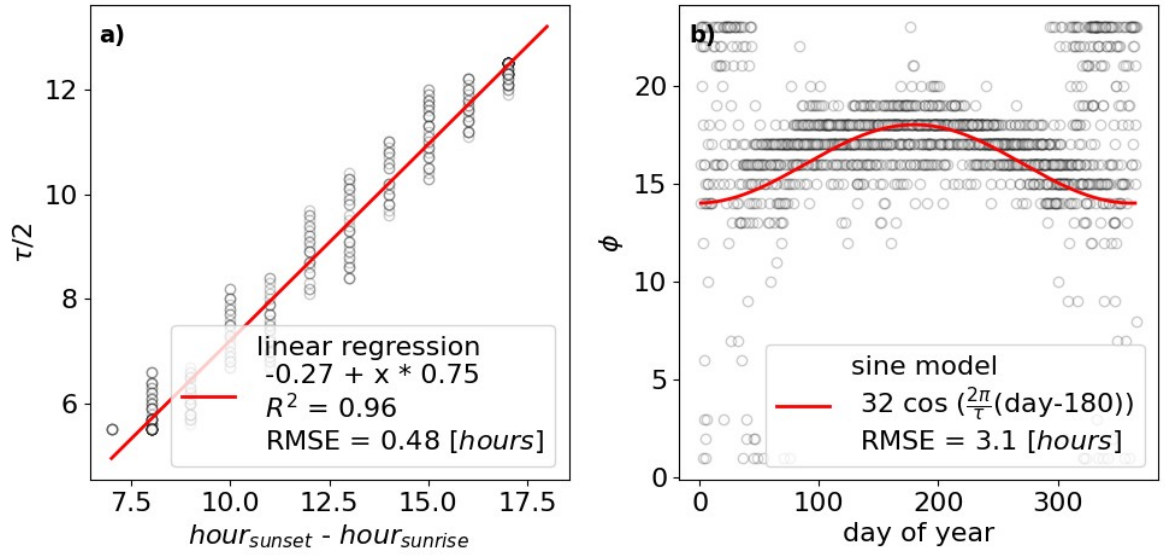

Figure S6. a) Transfer function to predict the time between dissolved oxygen (DO) minimum and maximum (τ/2) based on the hours between sunrise and sunset. b) Transfer function to predict the hour of maximum DO concentrations (ϕ) as a function of the day of the year. Circles show raw data from ~2000 days.

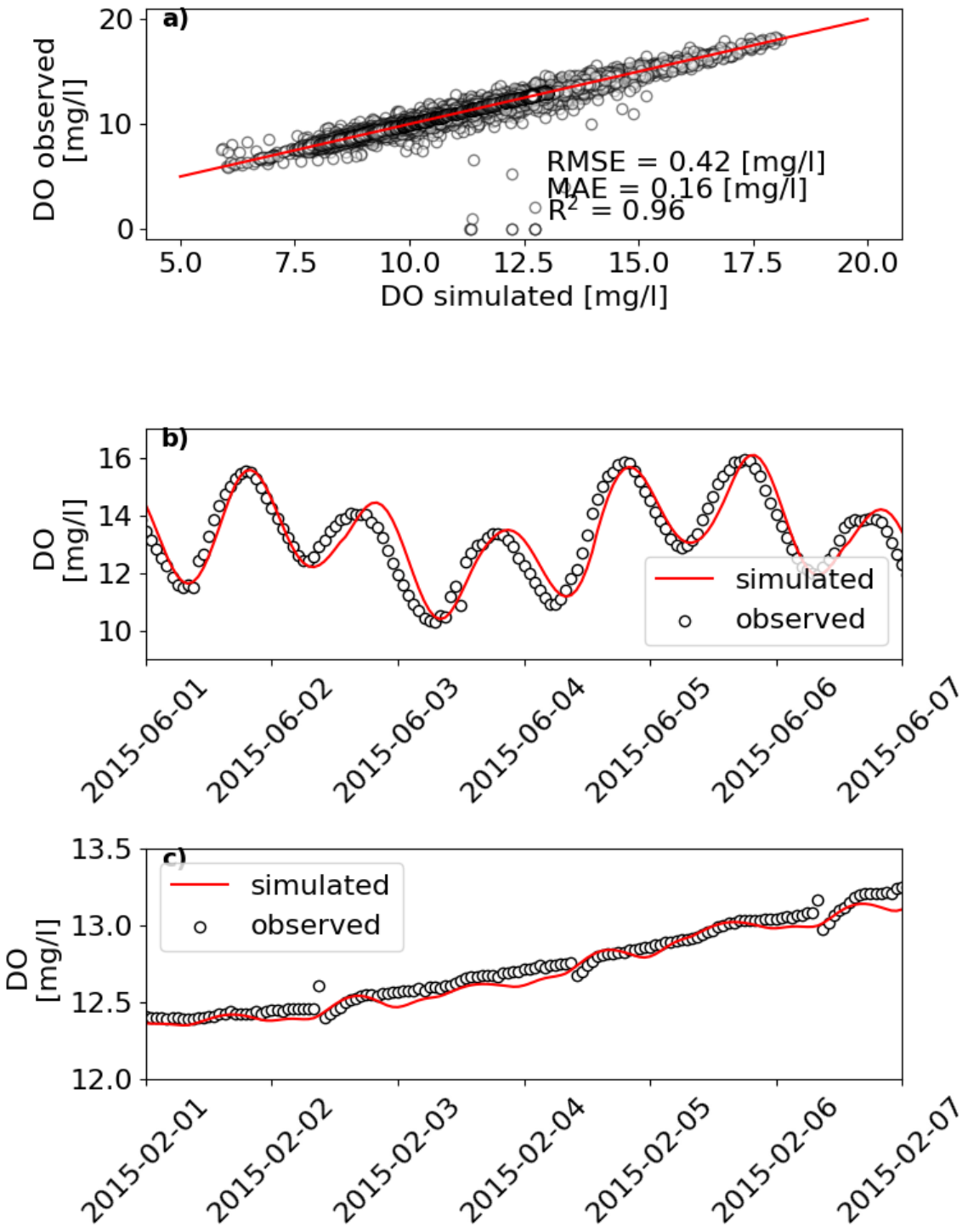

Figure S7. a) Scatter plot between predicted and observed 30 minute dissolved oxygen (DO) concentrations (aggreated to one hour) with the goodness of fit metrics root mean square error (RMSE), mean absolute error (MAE), and correlation coefficient R2. b) and c) show exemplary model fits during times with high (summer) and low (winter) daily variability in observed DO.

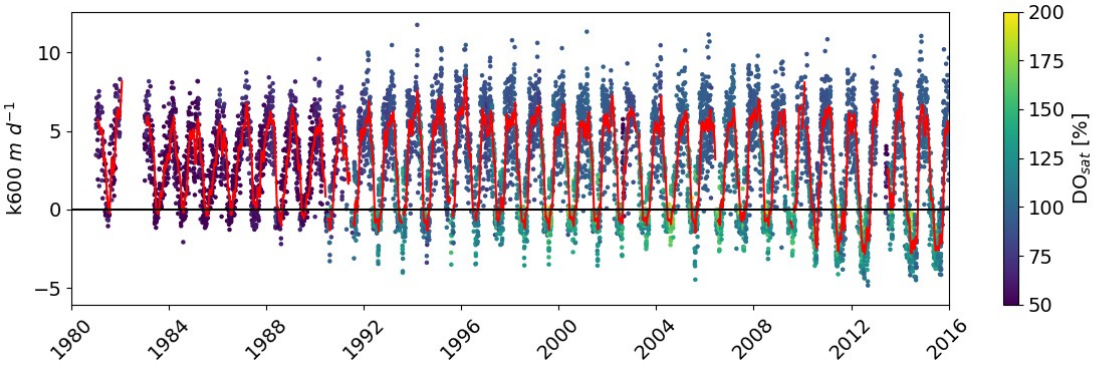

Figure S8: Time series of the modeled gas exchange rate (k600, see Eq. IV) for the investigated river segment. Colored points are actual fits and the red line represents a 30-day running mean. The color of the points represents the dissolved oxygen saturation of the river.

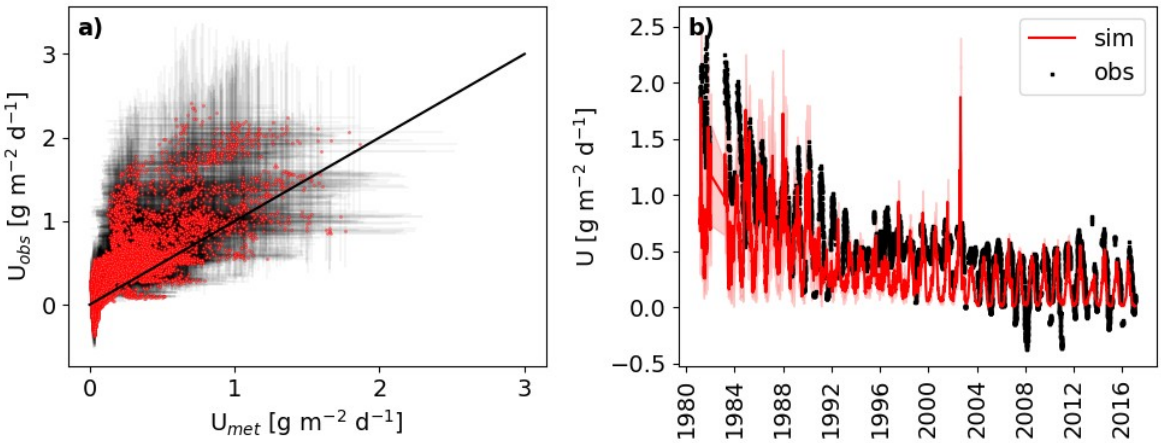

Figure S9: Simulated vs observed area-weighted dissolved inorganic nitrogen retention values (U)

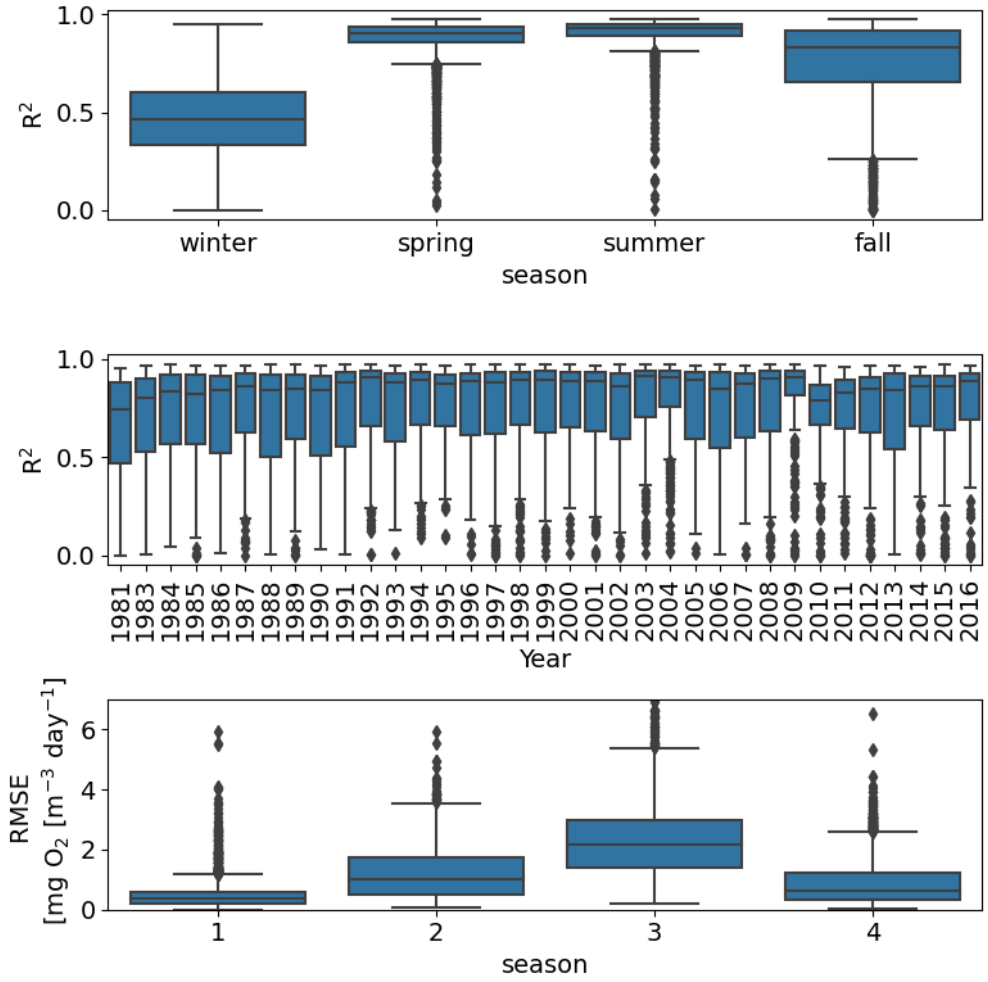

Figure S10: Goodness of fit metrics (correlation coefficient R^2, root mean square error RMSE) for the observed and simulated changes in dissolved oxygen concentration based on the Bayesian model. A) and c) shows the distribution over the season and b) over the entire time series.

6. Tables

Table 1. The goodness of fit metrics for different approaches of travel time corrections of the water quality time series. For the first three approaches, the outlet time series was shifted by n days as indicated. For the last approach, the travel time estimations were used to determine which shift (1 or 2 days) had to be applied. The root mean square error (RMSE), mean absolute error (MAE), and correlation coefficient R^2 were then computed by comparing the discharge in- and outflows.

	RMSE [m^3/s]	***MAE [m^3/s]***	***R^2***
0-day shift	73	44	0.99
1-day shift	53	33	0.99
2-day shift	66	38	0.99
τ-based shift	108	63	0.97

7. References

- Aberle, J., Nikora, V., Henning, M., Ettmer, B., Hentschel, B., 2010. Statistical characterization of bed roughness due to bed forms: A field study in the Elbe River at Aken, Germany. Water Resources Research 46. https://doi.org/10.1029/2008WR007406

- Arroita, M., Elosegi, A., Hall Jr., R.O., 2019. Twenty years of daily metabolism show riverine recovery following sewage abatement. Limnology and Oceanography 64, S77–S92. https://doi.org/10.1002/lno.11053

- Booker, D.J., Dunbar, M.J., 2008. Predicting river width, depth and velocity at ungauged sites in England and Wales using multilevel models. Hydrological Processes 22, 4049–4057. https://doi.org/10.1002/hyp.7007

- Chapra, S.C., Di Toro, D.M., 1991. Delta Method For Estimating Primary Production, Respiration, And Reaeration In Streams. Journal of Environmental Engineering 117, 640–655. https://doi.org/10.1061/(ASCE)0733-9372(1991)117:5(640)

- Correa-González, J.C., Chávez-Parga, Ma. del C., Cortés, J.A., Pérez-Munguía, R.M., 2014. Photosynthesis, respiration and reaeration in a stream with complex dissolved oxygen pattern and temperature dependence. Ecological Modelling 273, 220–227. https://doi.org/10.1016/j.ecolmodel.2013.11.018

- Gao, B., 1996. NDWI—A normalized difference water index for remote sensing of vegetation liquid water from space. Remote Sensing of Environment 58, 257–266. https://doi.org/10.1016/S0034-4257(96)00067-3

- Hall, R.O., Tank, J.L., Baker, M.A., Rosi-Marshall, E.J., Hotchkiss, E.R., 2016. Metabolism, Gas Exchange, and Carbon Spiraling in Rivers. Ecosystems 19, 73–86. https://doi.org/10.1007/s10021-015-9918-1

- Kamjunke, N., Rode, M., Baborowski, M., Kunz, J.V., Zehner, J., Borchardt, D., Weitere, M., 2021. High irradiation and low discharge promote the dominant role of phytoplankton in riverine nutrient dynamics. Limnology and Oceanography n/a.

https://doi.org/10.1002/lno.11778

- Modi, P., Revel, M., Yamazaki, D., 2022. Multivariable Integrated Evaluation of Hydrodynamic Modeling: A Comparison of Performance Considering Different Baseline Topography Data. Water Resources Research 58. https://doi.org/10.1029/2021WR031819

- Scharfe, M., Callies, U., Blöcker, G., Petersen, W., Schroeder, F., 2009. A simple Lagrangian model to simulate temporal variability of algae in the Elbe River. Ecological Modelling 220, 2173–2186. https://doi.org/10.1016/j.ecolmodel.2009.04.048